Robot-Aided Training of Propulsion: Effects of Torque Pulses Applied to the Hip and Knee Joint Under User-Driven Treadmill Control

Robert L. McGrath[1], *Member, IEEE,* and Fabrizio Sergi[1,2+], *Member, IEEE*

***Abstract*—We sought to establish whether torque pulses applied by an exoskeleton to the hip and knee joint modulate propulsion mechanics and whether changes in propulsion mechanics would be sustained after exposure to torque pulses under user-driven treadmill control. We applied twelve different formulations of torque pulses consecutively over 300 strides to 24 healthy participants, and quantified the evolution of four outcome measures – gait speed (GS), hip extension (HE), trailing limb angle (TLA), normalized propulsive impulse (NPI) – before, during, and immediately after training. We tested whether the pulse conditions modulated propulsion mechanics during and after training relative to baseline.**

Metrics of propulsion mechanics significantly changed both during and after training. After training, HE, NPI, and GS significantly increased in eleven conditions, three conditions, and four conditions, respectively.

Increases in HE during and after training were observed in conjunction with hip/knee flexion pulses during early stance, or hip/knee extension during late stance. Increases in NPI during training were associated with hip/knee extension during early stance, or knee flexion during late stance. Knee flexion during early stance resulted in positive after-effects in NPI. Increases in GS were associated with the application of hip flexion pulses.

Conditions exhibiting the largest positive changes in HE, and not NPI, during training resulted in increased GS after training. Analysis of the relationship between the effects measured during and after training suggests that, when present, after-effects arise from retention of training effects, and that retention is specific to the component of propulsion mechanics affected by training.

I. Introduction

Gait speed (GS) is a primary outcome measure in walking rehabilitation, as it indicates functional status [1] and it is associated with quality of life [2]. Walking includes three primary subtasks: propulsion, limb advancement, and body-weight support [3]. For propulsion, the trailing leg generates a forward oriented ground reaction force to accelerate the pelvis in the anterior direction [4], [5]. Early work examining GS and propulsion has determined that the GS increases with increased braking and propulsive impulses (integrated posterior and anterior ground reaction forces, respectively) [6]. Propulsion is determined by two components: 1) the plantarflexor moment generated about the ankle and 2) the trailing limb angle (TLA) [7]. The plantarflexor moment is generated primarily by the gastrocnemius and soleus muscles at late stance [8]. The trailing limb angle is the angle defined by the hip and foot landmark defined segment, relative to the vertical laboratory axis, commonly assessed at the moment of peak propulsive force [7], [9]–[14]. As such, propulsion can increase by applying a greater plantarflexor moment while keeping TLA constant, or by increasing TLA while applying the same plantarflexor moment. Due to the association between GS and propulsion, training methods that modulate the components of propulsion during walking are attractive for rehabilitation of individuals with neuromotor impairment [3].

Multiple methods have been developed for modulating propulsion mechanics during walking practice, such as wearable exoskeletons [15], [16], functional electrical stimulation combined with high-speed walking [12], challenge-based paradigms based on resistive forces applied by tethers to the pelvis [17] or arising from belt accelerations [11], and real-time biofeedback [18], [19]. Specifically, exoskeletons have been used to deliver torque to the hip and knee joint during stance, resulting in modulation of both components of propulsion in healthy participants [15]. Also, a soft exo-suit [20] has been developed to apply dorsiflexion and plantarflexion assistance during training to increase peak propulsive force, TLA, and therefore GS, in a hemiparetic subject [16]. Many other approaches based on exoskeletons, while not directly targeting propulsion mechanics, indirectly modulated propulsion mechanics while the exoskeleton controller was being optimized to minimize the cost of transport [21]–[23]. Functional electrical stimulation has been used to modulate propulsion mechanics extensively also in clinical popluations. As an example, patients post-stroke participating in a 12-week training protocol incorporating functional electric stimulation of paretic ankle dorsiflexor and plantarflexor musculature learned to generate clinically meaningful improvements in peak paretic propulsive force and increase TLA [12]. Finally, real-time biofeedback has been used to target changes in propulsion mechanics in healthy young and older adults [18], and a similar approach has been applied in post-stroke individuals, demonstrating the ability of post-stroke participants to increase paretic peak propulsive force through the two contributors of TLA and plantarflexor moment [24]–[26].

While most of the previous approaches demonstrated the ability of modulating propulsion mechanics during training, the ultimate goal of gait rehabilitation intervention is for beneficial effects to persist beyond training. However, the mechanisms of neuromuscular control involved in responding to interventions modulating propulsion mechanics are not well understood. Therefore, the effects of a training method on propulsion mechanics during and following training need to be both assessed and analyzed quantitatively.

This work was supported by the NSF-CBET-1638007

[1] Department of Biomedical Engineering, University of Delaware, Newark, DE 19713, USA

[2] Department of Mechanical Engineering, University of Delaware, Newark, DE 19713, USA

[+] Corresponding author - fabs@udel.edu

A specific challenge for studies targeting after-effects in propulsion mechanics is that these after-effects can not be quantified accurately in a standard treadmill setup based on fixed speed treadmill walking. For example, in our previous work, we applied torque pulses to the hip and knee joint during stance, and quantified the effects of pulsed torque application on propulsion mechanics both during and after exposure [15]. After exposure, the treadmill speed was fixed and equal to the one identified by the participant at baseline. Our previous setup was limited in studying after-effects of training on propulsion mechanics, as any intended effects on propulsion mechanics may be "cancelled" by the the constraint of walking at a constant, predetermined speed. In fact, hypothetical increases in propulsive force induced by training may not be "useful" for walking at that predetermined gait speed, which is identified in absence of any exoskeleton action. To properly evaluate the effects of exoskeletons on propulsion mechanics, it would be important to perform an evaluation during overground walking, or on a treadmill setup equipped to adjust the speed based on the intended speed of the participant [27].

In this work, we applied pulses of torque in consecutive strides to the knee and hip joints during stance while using a user-driven treadmill controller such that GS may change in response to changes in walking mechanics. We quantified propulsion kinematics with hip extension (HE), as measured by the robotic exoskeleton, and TLA as assessed by motion capture. Also, we quantified propulsion kinetics using NPI. We quantified effects during and after training in terms of the three outcome measures, plus GS resulting from the interaction between user, exoskeleton, and treadmill controller. We tested the primary hypothesis that any of the twelve pulse conditions modulate propulsion mechanics significantly during and after training relative to baseline. Moreover, we conducted secondary analyses to determine which parameters of the pulse conditions (i.e., joint torque, direction, timing) drove the effects during and after training, and to determine whether propulsion mechanics measured during pulsed torque training was associated with effects measured after training.

II. Methods

A. Study Participants & Pulse Conditions

We performed an a priori power analysis based on our previous study results [15] to determine sample size. We set α equal to 0.05/48 (corrected for 12 pulse conditions x 4 time point comparisons to baseline), β beta equal to 0.85, utilized two tailed statistics, and an effect size of 1.08 taken from the NPI outcome measure for pulse condition eight at the late assessment of after-effects that followed training. This analysis predicted a minimum sample size of 22 healthy participants to detect the targeted pre-post change in walking mechanics.

A subset of 12 pulse conditions were selected for testing to allow for a full factorial statistical assessment of pulse factors. However, exposing participants to all selected 12 pulse conditions would require more experimentation time than could reasonably be expected. As such, we divided participants into two groups and assigned two overlapping subsets of 8 pulses to each group (Fig. 1).

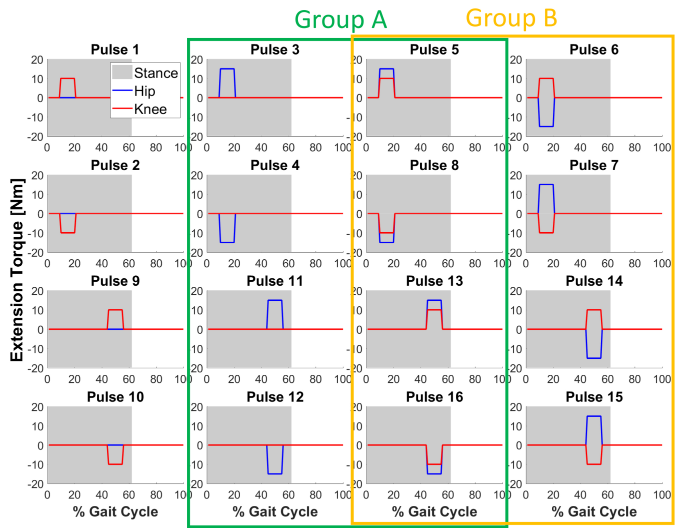

Fig. 1: Pulses corresponding to the two separate groups, each consisting of 11 participants.

This experiment included 22 healthy participants (12 males, 10 females), of age (mean $\pm$ std) 25.4 $\pm$ 4.8 yrs, height 173 $\pm$ 10 cm and mass 73.7 $\pm$ 17.5 kg. All participants were exposed to pulses 5, 8, 13, and 16, while only participants in Group A ($n = 11$) were exposed to pulses 3, 4, 11, and 12, and participants in Group B ($n = 11$) were exposed to pulses 6, 7, 14, and 15. Participants were only included if free of neurological and orthopedic disorders that affect normal walking function. All participants gave informed consent according to the IRB protocol number 929630 at the University of Delaware and wore their own comfortable lightweight athletic clothing.

B. Equipment

Data collections were conducted on an instrumented split-belt treadmill (Bertec Corp., Columbus OH, USA) that measured analog force/torque data. The ALEX II robot [28], a powered unilateral lower extremity exoskeleton, as seen in Fig. 2, was utilized to apply torque pulses about the right knee and hip joints of participants. The exoskeleton is suspended by a mobile carriage over the instrumented split-belt treadmill and secured from moving during experimentation by locking casters. Participants were protected from falling through the use of an overhead track and harness system (Solo-Step Inc., North Sioux City, SD, USA). A custom real-time controller written in MATLAB & Simulink (MathWorks Inc., Natick MA, USA) acquired signals from the instrumented split-belt treadmill and ALEX II and sent command signals to the two motors at a frequency of 1000 Hz.

The controller ran on two data acquisition multifunction I/O devices: PCIe-6321 and PCI-6221 which interfaced with Simulink through Quarc 2.6 (Quanser Consulting Inc, ON, Canada) on a Dell Precision 3620 with a Windows 7 OS (Dell Inc., Round Rock, TX, USA). The ALEX II contains two Kollmorgen ACM22C rotary motors with integrated Smart Feedback Devices (Danaher Corporation, Washington D.C., USA). These provide an emulated encoder resolution of 4096 pulses per revolution providing an effective hip and knee angle

Fig. 2: Experimental setup consisting of a participant in the Active Leg EXoskeleton II (ALEX II) and wearing a safety harness while on the instrumented split-belt treadmill.

resolution of $4.4 \cdot 10^{-4}$ deg. As in our previous work [15], the robot regulated the interaction forces at the cuffs using a feedback force controller that aimed to achieve the desired joint torque at the hip and knee, as prescribed by the specific torque pulse condition (Fig. 1).

C. User-driven Treadmill Controller

During experimentation, the speed of the treadmill belts were determined by the antero-posterior coordinate of the ALEX II suspension system. A T8-5805 rotary encoder (Kuebler Inc., NC, USA), located on one of the joints of four-bar mechanism of the ALEX II suspension system was read in real time by the Simulink control software. The software translated the real time encoder angle (θ_k) to a lunge position (D_k) quantified in meters via a calibration function with constant k_g. A proportional controller (gain G_k) was used to convert lunge distance (D_k) into to an increment in desired belt speed (V_{k+1}) at each iteration (k), at a rate of 1000 Hz.

$$
\begin{aligned}
&V_{k+1} = \mathrm{Avg}(V_{k-1000} : V_k) + G_k \cdot D_k \qquad (1)\\
&D_k = k_g \cdot (\sin(\theta_k) - \sin(\theta_0))[\mathrm{m}]\\
&G_k = 1.0[\mathrm{s}^{-1}], D_k > 0\\
&G_k = 1.5[\mathrm{s}^{-1}], D_k < 0
\end{aligned}
$$

The neutral lunge angle (θ_0) was calculated as the average of lunge encoder angle of eleven right and left gait cycles of walking at self-selected GS (ssGS). The current lunge angle (θ_k) was determined as the average lunge encoder angle over the past four strides. If the current lunge position (D_k) was anterior/greater or posterior/less than the neutral position/zero, the treadmill belt accelerated or decelerated, respectively. The treadmill belt velocities were controlled in real time by the Simulink program through a USB TCP/IP protocol connection with the treadmill control hardware.

D. Motion Capture

A ten camera T40-S (Vicon Motion Systems Ltd, Oxford, UK) system with Vicon Tracker 3.3 software was used to track the real time trajectories of two retroflective markers located on anatomical and robot landmarks. These two landmarks were the right malleoli and right hip joint center on the exterior of the exoskeleton hip linkage (inline with the shaft of the hip motor gearbox). The trajectories of these two markers were streamed in real time to Simulink with Vicon DataStream SDK 1.6 for logging and offline calculation of right TLA.

E. Experimental Procedures

1) Assessment Session: After fitting the exoskeleton to the participant, a first walking session was conducted to familiarize the participant with the exoskeleton, and with the assessment of ssGS and of the neutral lunge position. At the beginning of this session, the participant walked in the exoskeleton to assess the fit and alignment of the mechanism, followed by a couple of minutes for the participant to familiarize with the exoskeleton. Then, a second session was conducted to determine the participant's maximum safe GS while wearing the exoskeleton - up to the limit of 1.45 m/s. Next, the participant's ssGS was determined: three ramp-up (starting at 0.70 m/s and increased in increments of 0.05 m/s) and three ramp-down trials (starting at maximum safe GS and decreased in increments of 0.05 m/s) were performed, and each ended when the subject indicated having reached a comfortable speed. The average of these six trials, which we considered to be the ssGS, was set as the starting treadmill speed for all pulse training sessions. After determining ssGS, the neutral lunge position of the participant was assessed. Utilizing the acquired neutral lunge position, the participant was given 200 strides to explore the behavior of the user-driven treadmill speed controller via antero-posterior lunge.

2) Pulse Training Sessions: In the first visit, the participant proceeded to perform the first two training sessions. Training sessions were performed entirely under user-driven treadmill control and consisted of 100 or 150 strides of transparent control for baseline assessment, 300 strides of pulsed-torque training (utilizing one of the eight pulse conditions), and 200 strides of after-effect assessment. The first 9 participants and last 13 participants were exposed to 100 and 150 strides of baseline, respectively. The number of strides at baseline were increased after seeing inconsistent convergence across the first 9 participants to a steady state value after 100 strides. Each session lasted for approximately 15 minutes and all sessions within the same visit were separated by a minimum of 10 minutes of rest outside of the exoskeleton to reduce the effects of fatigue. The second and third visits each consisted

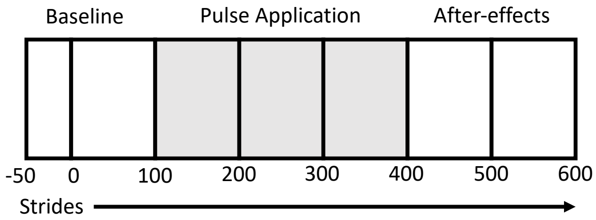

Fig. 3: Visual representation of a training session, consisting of 100 (or 150) strides of baseline, 300 strides of pulse application, followed by 200 strides for after-effect assessment.

of 3 additional pulse training sessions, for a total of eight pulse training sessions. The order of assignment of pulse conditions to training sessions were pseudo-randomized across participants.

F. Data Analysis

For this experiment, out of the 176 total trials (8 sessions from 22 participants), 3 were not included in final data analysis. One trial was excluded due to operator error in saving the data, a second trial was excluded due to equipment malfunction, and a third trial was excluded due to premature termination as the participant reported discomfort due to interaction with that particular pulse condition. Furthermore, a total of 7 training sessions in which GS became saturated (reached the upper limit of 1.45 m/s) during baseline were excluded from the analysis.

1) Outcome Measures: Four outcome measures were selected to describe the effects of the intervention on propulsion mechanics, defined consistent with our previous work [15] (when applicable). Gait speed (GS) was defined as the velocity of the two treadmill belts, as determined by the response of user-driven treadmill controller. Right hip extension angle (HE) was defined as the angle of the hip of the right (robot-assisted) leg as measured by the hip motor encoder at the instant of peak anterior ground reaction force (aGRF). Normalized propulsive impulse (NPI) of the right leg was defined as the integral of the antero-posterior component of GRF over the time interval that the component is positive, normalized by the participant's body weight (in N). Trailing limb angle of the right leg (TLA) was defined as the angle formed by the line connecting the hip marker and ankle marker (V_{Leg}), relative to the global vertical axis, at the instant (t_P) of peak aGRF, i.e., as:

$$\begin{aligned} TLA &= \mathtt{atan2}(V_{Leg}(2), V_{Leg}(3)) \qquad (2)\\ V_{Leg} &= [X_{Hip}, Y_{Hip}, Z_{Hip}] - [X_{Ank}, Y_{Ank}, Z_{Ank}] \end{aligned}$$

The experiment was divided into three sections: 100 strides before pulse application (baseline), 300 strides of pulse application, and 200 strides following pulse application. To perform statistical analysis, we defined five time points of measurement (TP): baseline (BL) - last 20 strides before intervention (strides 81-100), early pulse application (P-E) - strides 2-21 after start of intervention (102-121), late pulse application (P-L) - last 20 strides of intervention (381-400), early after-effects (AE-E) - strides 2-21 after the end of intervention (402-421), and late after-effects (AE-L) - last 20 strides of no pulse condition after intervention (581-600). At each of these time points, we obtained the outcome measure as the mean for the designated strides.

2) Effects of torque pulses on propulsion mechanics: We performed pairwise tests to establish whether any pulse condition significantly modulated the outcome measures during pulse application (2 paired tests per pulse pairing P-E with BL and P-L with BL), and after pulse application (2 paired tests per pulse pairing AE-E with BL and AE-L with BL). The Shapiro-Wilk test was used to detect normality of the paired samples. If the samples were normally distributed, a t-test was performed, otherwise a Wilcoxon signed-rank test was performed. For either test, a false-positive rate of $\alpha = 0.05/48$ was selected, using a Bonferroni correction to account for 48 comparisons (4 comparisons per pulse x 12 pulses). Since the Bonferroni correction leads to a conservative statistical threshold, we also report the significance of pulse-specific Dunnett's tests for comparison of outcomes at each Time Point relative to baseline, within each pulse condition of each measure, given a false-positive rate of $\alpha = 0.05/4$.

3) Effects of torque pulse parameters on propulsion mechanics: We performed linear mixed effect models to determine how factors of the pulses modulated the outcomes at different time points. We utilized JMP Pro Version 16 (SAS Institute Inc., Cary, NC, USA) to fit a linear mixed model to each of the four outcome measure data sets consisting of 880 data points. Each data set consisted of 2 groups, 11 participants per group, 8 pulse conditions per participant group (of the 12 total pulse conditions), 5 evaluation time points per pulse condition, and one outcome per time point. The linear mixed model effects were participant (1 through 22), phase of gait cycle (Early or Late Stance), hip torque (-15 N·m or 15 N·m, respectively), knee torque (-10 N·m, 0 N·m, or 10 N·m), and time point of measurement (BL, P-E, P-L, AE-E, or AE-L). The fixed effects included the main, two-way, three-way, and four-way effects of stance, knee torque, hip torque, and time point. The random effects included the main effect of participant and two-way interaction of participant and the four main effects. Fixed effects tests and statistical contrasts were conducted with a false positive rate of $\alpha = 0.05$.

4) Association between propulsion mechanics during and after torque pulse application: Stepwise regressions were performed on the measured data to establish the association between the change in measured effects from baseline (BL) to late after training (AE-L) (dependent variable) and the change in effects measured between BL and training (P-E & P-L) across all pulse condition and participants (set of independent variables). Given the multi-collinearity problem in the multiple metrics of propulsion mechanics quantified during training, we used a stepwise regression method to identify a minimal set of explanatory variables for each outcome measure [29], and ran separate models for each of the four outcomes. The initial terms considered for each model included the difference in effects of all four outcome measures assessed between BL and training (P-E & P-L). For each of the four models, we performed a stepwise regression with backward elimination, utilizing an automatic exclusion rule of $p < 0.05$ to remove explanatory variables from the models. The backwards elimination procedure was given freedom to select terms regardless of broken hierarchy.

III. Results

The stride by stride group means, with the BL Time Point value subtracted, of the four outcome measures for all twelve pulses are visualized in Figs S1 - S4. The results of statistical analysis conducted using the selected outcome measures is reported below.

A. Effects of torque pulses on propulsion mechanics

Table I lists the effect sizes of change of each outcome measure relative to baseline, at each time point of measurement. The outcomes are visible in Fig. 4, broken down by experimental factor. Results are discussed below, separately for each outcome measure. In the text below, the Dunnett's correction is used to determine statistical significance for the effects of individual pulses, allowing for a more thorough reporting.

1) Gait Speed: GS did not change significantly relative to baseline at early pulse application in any pulse condition. At late pulse application, GS increased in four conditions (Pulses 4, 8, 12, and 16, range of change: 0.059±0.017 m/s – 0.099±0.023 m/s, $p \leq 0.005$). At early after-effects, GS remained above baseline in two conditions (Pulses 4 and 8, r.o.c.: 0.063±0.017 m/s – 0.076±0.028 m/s, $p \leq 0.030$). At late after-effects, GS remained above BL for these two conditions and increased relative to baseline for two additional conditions (Pulses 4, 8, 14 and 16, r.o.c.: 0.063±0.017 m/s – 0.074±0.028 m/s, $p \leq 0.037$). Overall, a mean positive (though not always significant) after-effect was detected for change in GS relative to baseline in eleven out of twelve conditions.

2) Hip Extension: At early pulse application, HE decreased relative to baseline in two conditions (Pulses 5 and 16, r.o.c.: -2.312±0.853 deg – -3.958±0.859 deg, $p \leq 0.029$), and increased in one condition (Pulse 4, change: 2.357±0.912 deg, $p = 0.0481$). At late pulse application, HE was greater than baseline in eight conditions (Pulses 4, 6, 7, 8, 11, 13, 14, and 15, range of change: 2.464±0.812 deg – 6.669±0.971 deg, $p \leq 0.036$). During both early and late after-effects, HE was greater than baseline in eleven conditions (all except Pulse 12) (range of change: 2.378±0.812 deg – 5.926±0.971 deg, $p \leq 0.034$).

3) Normalized Propulsive Impulse: At early pulse application, NPI decreased relative to baseline in two conditions (Pulses 8 and 14, r.o.c.: -2.769±0.947 ms – -3.188 ±1.079 ms, $p \leq 0.020$), and increased in two conditions (Pulses 5 and 15, range of change: 3.609±0.710 ms – 5.781±1.160 ms, $p < 0.001$). At late pulse application, NPI remained lower than baseline in one condition (Pulse 14, change: -3.244±1.08 ms, $p = 0.017$), and remained higher than baseline in one condition (Pulse 15, change: 4.184±0.710 ms, $p < 0.001$), respectively. During early after-effects, NPI increased in three conditions relative to baseline (Pulses 8, 13, and 7, r.o.c.: 2.136±0.776 ms – 2.771±0.9039 ms, $p \leq 0.022$), and remained greater than baseline only in one of these conditions (Pulse 13, change: 2.462±0.7585 ms, $p = 0.007$).

4) Trailing Limb Angle: At early pulse application, TLA increased relative to baseline in one condition (Pulses 4, change: 0.996±0.290 deg, $p = 0.006$), and remained greater than baseline at late pulse application (change: 1.139 ±0.290 deg, $p = 0.002$). At early pulse application, TLA decreased relative to baseline in one condition (Pulse 5, change: -0.966±0.380 deg, $p = 0.045$). No significant changes in TLA relative to baseline were measured after pulse application.

B. Effects of torque pulse parameters on propulsion mechanics

The linear mixed effect models had an adjusted R^2 of 0.70, 0.71, 0.86, and 0.76 for GS, HE, NPI, and TLA, respectively, which indicates a high goodness of fit. The fixed effects are reported in Table II. Given the interest in analyzing training effects, the significant fixed effects that include TP are presented in detail below, together with a list of relevant post-hoc tests that are useful to interpret the size and direction of each effect.

1) Gait Speed: Time Point was a significant main effect for GS, as GS was greater at P-L (0.034±0.012 m/s, $p = 0.043$), AE-E (0.034±0.012 m/s, $p = 0.039$), and AE-L (0.047±0.012 m/s, $p = 0.002$) than BL, across all pulse conditions.

Also, the model revealed a significant interaction of Time Point and Hip Torque, shown in Fig. 5, driven by an increase in GS at P-L (0.067±0.016 m/s, $p = 0.001$) and AE-L (0.062±0.016 m/s, $p = 0.005$) from BL, under the application of Hip Flexion Torque. A contrast analysis of this two-way interaction shows that the change in GS between P-L and BL was greater under Hip Flexion Torque than under Hip Extension Torque (0.067±0.010 m/s, $p = 0.001$).

2) Hip Extension: Time Point was a significant main effect for HE, as HE was greater at P-L (2.66±0.48 deg, $p < 0.001$) and P-E (2.78±0.48 deg, $p < 0.001$) than BL. At Time Point AE-E, HE was greater than BL (3.72±0.48 deg, $p < 0.001$) and P-E (3.84±0.48 deg, $p < 0.001$). Lastly, HE at Time Point AE-L was greater than BL (4.50±0.48 deg, $p < 0.001$), P-E (4.61±0.48 deg, $p < 0.001$), and P-L (1.84±0.48 deg, $p = 0.002$).

The three-way interaction of Time Point, Phase, and Knee Torque was significant for HE (Fig. 6). For Knee Flexion Torque pulses at Early Stance, HE increased at several Time Points compared to BL (P-L: 3.93±0.93 deg, $p = 0.009$, AE-E: 4.54±0.93 deg, $p < 0.001$, and AE-L: 4.43±0.93 deg, $p < 0.001$). Similarly, for Knee Extension Torque pulses at Late Stance, HE increased at several Time Points compared to BL (P-L: 4.60±0.93 deg, $p < 0.001$, AE-E: 4.83±0.93, $p < 0.001$, AE-L: 5.76±0.93 deg, $p < 0.001$). For Knee Extension Torque pulses at Early Stance, HE was greater at AE-L than BL (4.37±0.93 deg, $p = 0.001$) and similarly for Knee Flexion Torque at Late Stance, HE was greater at AE-L than BL (4.28±0.93 deg, $p = 0.002$). Lastly, in conditions Zero Knee Torque pulses at Early Stance conditions (grouping conditions where only hip torque is applied at Early Stance, i.e. Pulses 3 and 4), HE was greater at AE-L than BL (5.32±1.15 deg, $p = 0.002$).

TABLE I: Effect sizes for all pairwise comparisons between baseline and each following time points for all twelve conditions. Values are bolded if statistically significant using a Bonferroni correction across all pulses, and marked with an asterisk if significant for a pulse-specific Dunnett's test.

Measure	TP	P3	P4	P5	P6	P7	P8	P11	P12	P13	P14	P15	P16
GS	P-E	-0.86	0.55	-0.52	**-1.51**	-0.11	0.19	-0.13	0.42	0.00	0.26	0.76	0.58
	P-L	-0.29	0.91*	-0.25	0.44	0.10	0.74*	-0.08	0.70*	0.00	0.21	0.27	**0.95***
	AE-E	-0.13	1.21*	0.03	0.51	0.20	0.54*	0.19	0.61	0.28	0.17	0.29	0.39
	AE-L	-0.10	0.90*	0.29	0.60	0.02	0.52*	0.33	0.20	0.48	0.88*	0.46	0.59*
HE	P-E	-0.74	0.92*	**-1.67***	0.00	-0.33	0.08	0.71	-0.71	0.68	-0.48	**2.45**	-0.59*
	P-L	0.39	**1.42***	-0.20	0.78*	1.11*	**1.55***	0.96*	0.05	**1.35***	0.90*	**1.64***	-0.29
	AE-E	**1.62***	**1.92***	**1.17***	0.75*	**2.09***	**1.47***	1.15*	0.65	**1.38***	1.46*	**1.68***	0.78*
	AE-L	**1.50***	1.33*	**0.88***	1.05*	1.07*	**1.47***	0.72*	0.62	**1.05***	1.49*	1.30*	**0.99***
NPI	P-E	0.99	-0.50	**0.89***	0.67	0.24	-0.58*	1.12	-0.59	-0.49	-1.83*	**2.29***	0.86*
	P-L	0.50	-0.54	0.55	0.50	0.66	0.15	-0.01	-0.25	-0.06	-0.67*	1.45*	0.21
	AE-E	-0.11	0.30	-0.81	0.51	1.37*	**0.86***	0.47	0.33	0.65*	0.16	0.74	-0.11
	AE-L	0.58	0.21	0.03	0.45	0.65	0.69	0.33	0.30	0.68*	0.72	0.56	0.39
TLA	P-E	-0.38	0.96*	-0.56*	-0.27	0.00	0.27	-0.40	0.07	-0.38	-0.92	0.46	0.21
	P-L	-0.28	0.76*	-0.50	0.08	-0.03	0.63	-0.36	0.25	-0.20	-0.49	0.41	0.33
	AE-E	0.02	0.91	0.32	0.43	0.22	0.41	-0.06	0.36	0.14	-0.04	0.57	0.41
	AE-L	-0.14	0.40	0.05	0.32	-0.12	0.40	0.01	-0.01	0.17	0.75	0.45	0.36

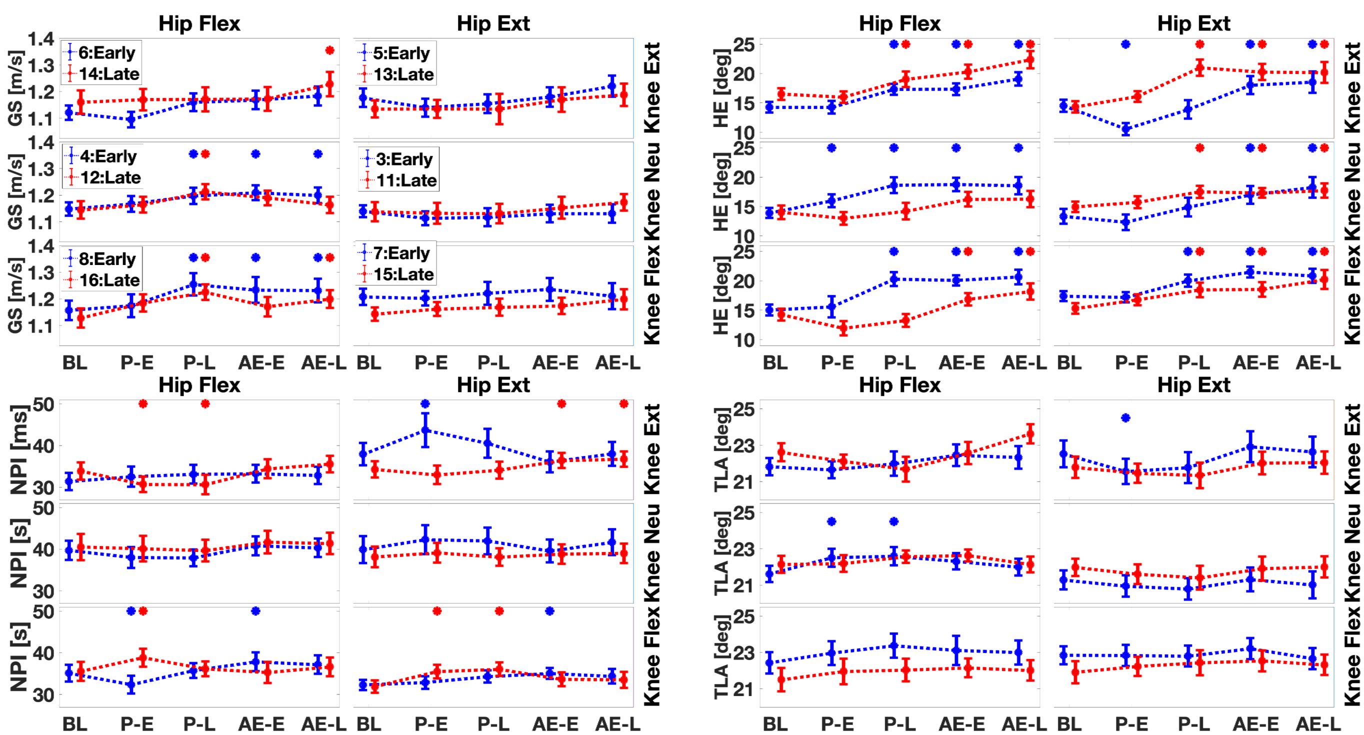

Fig. 4: Breakdown of GS, HE, NPI, and TLA by factor for the twelve tested pulses. Circles indicate measured group means, whiskers indicate s.e.m., asterisks indicate statistically significant Dunnett's test comparison to respective baseline.

A contrast analysis of the three-way interaction of Time Point, Phase, and Knee Knee Torque revealed that for Early Stance pulses, a change from Flexion to Extension Torque at the Knee decreased HE (-2.688±0.618 deg, $p = 0.030$) at P-L relative to BL. Conversely, for Late Stance pulses, a change from Flexion to Extension Torque at the Knee increased HE (3.534±0.622 deg, $p = 0.005$) at P-L relative to BL.

The three-way interaction of Time Point, Phase, and Hip Torque was significant for HE (Fig. 7). For Hip Flexion Torque pulses at Early Stance, HE was greater at several Time Points compared to BL (P-L: 4.42±0.82 deg, $p < 0.001$, AE-E: 4.18±0.82 deg, $p < 0.001$, AE-L: 5.07±0.82 deg, $p < 0.001$). Similarly, for Hip Extension Torque pulses at Late Stance, HE increased at several Time Points compared to BL (P-L: 4.13±0.82 deg, $p < 0.001$, AE-E: 3.85±0.82 deg, $p < 0.001$, AE-L: 4.53±0.82 deg, $p < 0.001$). For Hip Extension Torque pulses at Early Stance, HE was greater at AE-E (3.98±0.82 deg, $p < 0.001$) and AE-L (4.35±0.82 deg, $p < 0.001$) relative to BL. Lastly, for Hip Flexion Torque pulses at Late Stance, HE at AE-L was greater than BL (4.06±0.85 deg, $p < 0.001$).

A contrast analysis of the three-way interaction of Time Point, Phase, and Hip Torque revealed that for Hip Flexion

TABLE II: Fixed effect test results for the linear mixed effect models: GS, HE, NPI, and TLA

GS Fixed Effects Tests	Nparm	DFNum	DFDen	F Ratio	Prob >F
TP	4	4	97.9	5.895	<0.001
TP·Hip Trq	4	4	570.4	2.605	0.035
Phase·Knee Trq	2	2	553.2	3.689	0.026
Knee Trq·Hip Trq	2	2	183.4	4.622	0.011
HE Fixed Effects Tests	**Nparm**	**DFNum**	**DFDen**	**F Ratio**	**Prob >F**
TP	4	4	97.6	38.677	<0.001
Phase·Knee Trq	2	2	520.2	41.298	<0.001
TP·Phase·Knee Trq	8	8	564.3	2.151	0.030
Phase·Hip Trq	1	1	576.9	14.294	<0.001
TP·Phase·Hip Trq	4	4	564.36	6.620	<0.001
NPI Fixed Effects Tests	**Nparm**	**DFNum**	**DFDen**	**F Ratio**	**Prob >F**
TP	4	4	104.7	2.482	0.048
Phase·Knee Trq	2	2	578.0	7.791	<0.001
TP·Phase·Knee Trq	8	8	577.1	7.380	<0.001
TP·Hip Trq	4	4	577.6	4.246	0.002
Phase·Hip Trq	1	1	584.4	34.965	<0.001
Phase·Knee Trq·Hip Trq	2	2	593.6	6.181	0.002
TLA Fixed Effects Tests	**Nparm**	**DFNum**	**DFDen**	**F Ratio**	**Prob >F**
TP·Knee Trq	8	8	575.9	2.306	0.020
Phase·Knee Trq	2	2	565.0	5.160	0.006
Knee Trq·Hip Trq	2	2	82.9	4.932	0.010
Phase·Knee Trq·Hip Trq	2	2	584.7	5.583	0.004

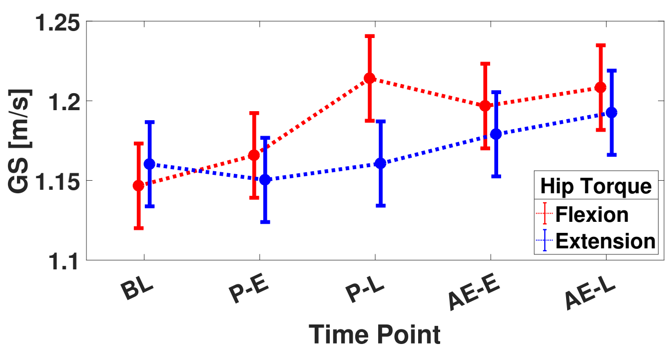

Fig. 5: Least square means and S.E.M. of the two-way interaction between Time Point and Hip Torque of the linear mixed model for GS.

Torque pulses, a change from Early to Late Stance decreased HE (-3.67±0.554 deg, $p = 0.001$) at P-L relative to BL. Conversely, for Hip Extension Torque pulses, a change from Early to Late Stance increased HE at P-E (3.000±0.546 deg, $p = 0.006$) and at P-L (2.784±0.546 deg, $p = 0.010$), relative to BL.

3) Normalized Propulsive Impulse: Time Point was a significant main effect for NPI, as NPI was greater at AE-L than BL (1.32±0.44 ms, $p = 0.025$) across all conditions. The model revealed a significant interaction of Time Point and Hip Torque (Fig. 8). This was driven by a greater increase of NPI from BL, at P-E and P-L, under Hip Extension Torque pulses relative to Hip Flexion Torque (P-E: 2.51±0.46 ms, $p = 0.007$; P-L: 2.34±0.46 ms, $p = 0.011$).

The three-way interaction of Time Point, Phase, and Knee Torque was significant for NPI (Fig. 9). A contrast analysis shows that within the Early Stance Phase condition, with respect to BL, a change from Knee Flexion Torque to Knee

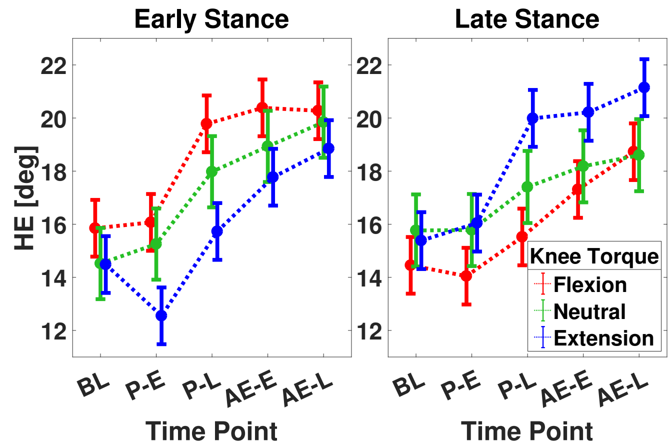

Fig. 6: Least square means and S.E.M. of the three-way interaction between Time Point, Phase, and Knee Torque of the linear mixed model for HE.

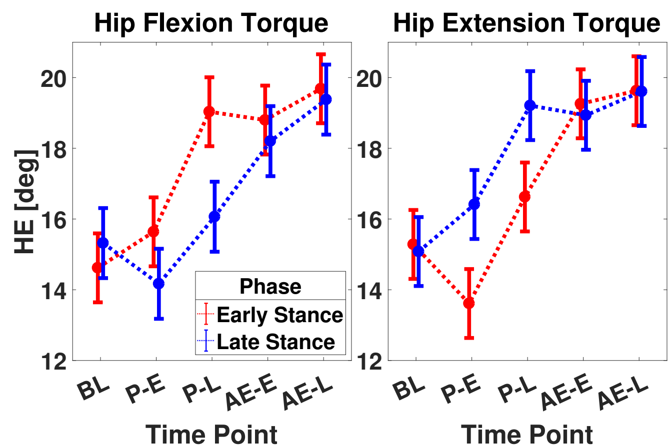

Fig. 7: Least square means of the three-way interaction between Time Point, Phase, and Hip Torque of the linear mixed model for HE.

Extension Torque yields an increase in NPI (4.56±0.73 ms, $p = 0.002$) at P-E. Conversely, within the Late Stance Phase condition, with respect to BL, a change from Knee Flex Trq to Knee Ext Trq yields a decrease in NPI at P-E (-5.68±0.74 ms, $p < 0.001$) and P-L (-4.10±0.74 ms, $p = 0.005$).

4) Trailing Limb Angle: The two-way interaction between Time Point and Knee Torque was significant for TLA. A contrast analysis reveals that the change in TLA with respect to BL under Knee Flexion Torque is greater than the one measured under Knee Extension Torque at two time points (P-E: 0.822±0.177 deg, $p = 0.021$); P-L: 0.982±0.177 deg, $p = 0.006$).

C. Association between propulsion mechanics during and after torque pulse application

The stepwise regression models identified robust associations between changes in propulsion mechanics during and after torque pulse application, with R^2 values of 0.46, 0.51, 0.26, and 0.38 for GS, HE, NPI, and TLA, respectively. For GS, only two terms remained in the model after backwards elimination, while three terms remained in the models for HE, NPI, and

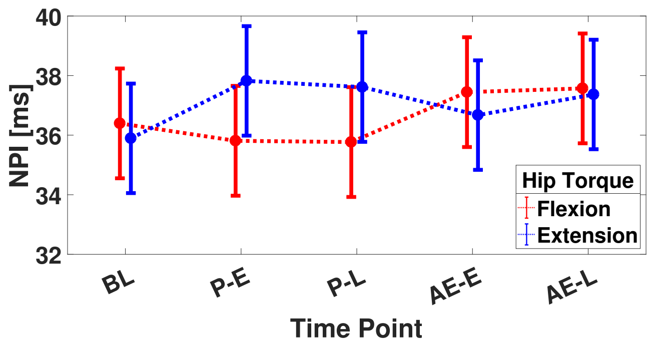

Fig. 8: Least square means and S.E.M. of the two-way interaction between Time Point and Hip Torque of the linear mixed model for NPI.

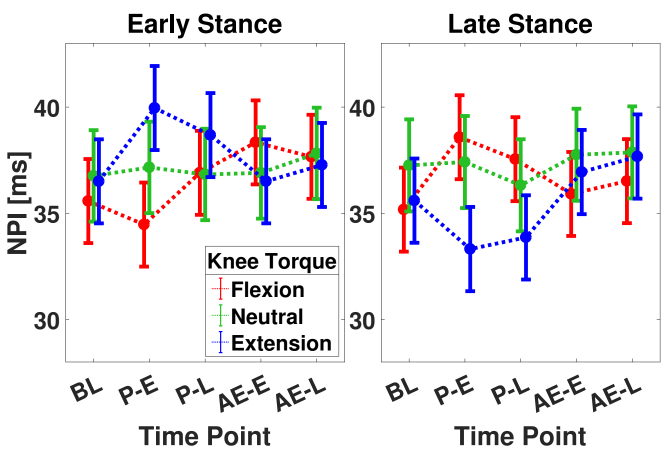

Fig. 9: Least square means and S.E.M. of the three-way interaction between Time Point, Phase, and Knee Torque of the linear mixed model for NPI.

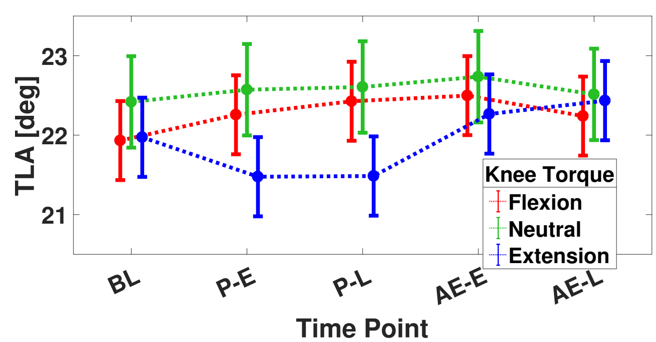

Fig. 10: Least square means and S.E.M. of the two-way interaction between Time Point and Knee Torque of the linear mixed model for TLA.

TABLE III: Fixed effects test results for the stepwise regression models: GS, HE, NPI, and TLA

GS AE-L	**Estimate**	**t Ratio**	**Prob >F**
GS P-L	0.701	143.36	<0.001
TLA P-E	-0.010	4.72	0.031
HE AE-L	**Estimate**	**t Ratio**	**Prob >F**
HE P-L	0.787	165.00	<0.001
HE P-E	-0.392	25.59	<0.001
GS P-E	8.807	5.75	0.018
NPI AE-L	**Estimate**	**t Ratio**	**Prob >F**
NPI P-L	0.378	43.81	<0.001
NPI P-E	-0.160	9.05	0.003
HE P-L	0.141	52.55	0.006
TLA AE-L	**Estimate**	**t Ratio**	**Prob >F**
TLA P-L	0.547	84.66	<0.001
TLA P-E	-0.237	6.94	0.009
GS P-E	4.247	5.25	0.023

TLA, a large reduction from the initial set of 8 explanatory variables. Measurements of the same outcome during pulse application were consistently retained by the backwards elimination procedure, for all outcomes. Specifically, a consistent positive association between the measurement of a specific outcome at P-L and the measurement of the same outcome at AE-L was detected in all models as the term with the highest level of significance. This association can be interpreted as a retention of the effects of training, where for GS, 70% of the changes measured at P-L were retained at AE-L (parameter estimate: 0.701, t-ratio: 143.36); for PE, 79% of the changes measured at P-L were retained at AE-L (parameter estimate: 0.787, t-ratio: 165.00); for NPI, 38% of the changes measured at P-L were retained at AE-L (parameter estimate: 0.378, t-ratio: 43.81); for TLA, 55% of the changes measured at P-L were retained at AE-L (parameter estimate: 0.547, t-ratio: 84.66) (S5, column one).

Secondary to the retention effects, the model also identified a negative association between changes in propulsion mechanics during early pulse application and after-effects (S5, column two). Specifically, 40% of the changes in HE at P-E were reflected in the opposite direction at AE-L (parameter estimate: -0.392, t Ratio: 25.69), 16% of the changes in NPI at P-E were reflected in the opposite direction at AE-L (parameter estimate: -0.160, t Ratio: 9.05), and 23% of the changes in TLA at P-E were reflected in the opposite direction at AE-L (parameter estimate: -0.237, t Ratio: 6.94). For GS, the term that remained in the model was TLA P-E (positively associated with GS at P-E, $r = 0.66$), also with a significant negative association (parameter estimate: -0.01 m/s/deg, t Ratio: 4.72). Other terms that remained in the stepwise regression models were changes in GS during early pulse application (positively associated with both HE and TLA, t Ratio: 5.75 and 5.25, respectively), and changes in HE in late pulse application (positively associated with NPI AE-L, t Ratio: 52.55).

IV. Discussion

The main objective of this experiment was to quantify the effects on propulsion mechanics of torque pulses applied to the hip and knee joint during the stance phase of walking, when participants walk on a user-driven treadmill. We collected data on 22 healthy participants, exposed to twelve different combinations of torque pulses, applied to the hip and/or knee joint during early or late stance, and quantified the effects on propulsion mechanics, specifically gait speed (GS), hip extension (HE), normalized propulsive impulse (NPI), and trailing limb angle (TLA).

Overall, our experiment indicates that pulses of torque applied to the hip and knee joint during user-driven treadmill control can induce significant changes in propulsion mechanics in a group of healthy individuals. The most consistent effects were measured for the outcome measure of HE. HE increased significantly during pulse application in eleven out of twelve conditions, and decreased relative to baseline in two conditions during early pulse application. Moreover, HE increased after training relative to baseline in eleven out of twelve pulse conditions. Significant effects during and after pulse application were detected also for NPI, with significant positive or negative changes measured during pulse application (five out of twelve conditions), and significant increases in NPI measured in three of twelve conditions after torque pulse application. Effects on GS were present in a smaller number of conditions than in HE (positive effect in eight out of twelve conditions at late pulse application), but changes in GS were positively associated with changes in HE at all time points (r regression coefficient at PE-E: 0.41, PE-L: 0.22, AE-E: 0.35, AE-L: 0.40), more so than with changes in NPI (r regression coefficient at PE-E: 0.09, PE-L: 0.00, AE-E: 0.17, AE-L: 0.11). Effects on TLA were also associated with the effects on HE (r regression coefficient at PE-E: 0.63, PE-L: 0.43, AE-E: 0.37, AE-L: 0.48), but the magnitude of the effects on TLA was much smaller than on HE (significantly increased relative to baseline only in one pulse condition during training, no significant changes in TLA were detected after training).

Phase was the most important factor in modulating HE effects during and after training, relative to baseline, as knee torque and hip torque modulated HE differently, and often in opposite directions, depending on the timing of the applied pulse. For example, at P-L, knee torque applied in flexion or extension exhibited an opposite change in HE with respect to BL, depending on whether the torque was applied during early or late stance. Similarly, at each hip torque condition, a reversal in phase condition lead to a different directional change in HE with respect to BL. Ultimately, the kinematic measure of interest for propulsion is TLA. Our analysis indicates that pulses of torque to the hip and knee have only a limited effect on modulating TLA, suggesting likely compensations occurring with the ankle joint and possibly with the timing of push-off. This observation is consistent with the literature that HE angle is not directly related to propulsion mechanics [30].

For NPI, a kinetic measure of propulsion, pulse application effects were positive for 2 of 12 conditions and negative in 1 of 12 conditions in direction, followed by positive after-effects in 3 conditions. There was an effect of hip torque on NPI measured during pulse application, where HE increased NPI more than hip flexion, regardless of pulse timing. There was also a different effect of NPI for a change in knee torque depending on the timing of the delivered pulse. When the pulse was applied at early stance, a change from flexion to extension knee torque increased NPI at P-E but decreased NPI at P-E for late stance. For after-effects, knee flexion during early stance resulted in positive after-effects in NPI.

One goal of the experiment was to establish whether any effects in propulsion mechanics translated to an increase in GS in a user-driven treadmill condition. GS exhibited significant effects only for conditions of hip flexion torque, and all significant effects during pulse application and after-effects were positive in direction. In general, conditions exhibiting the largest positive changes in HE, and not NPI, during or after training resulted in increased GS after training. For example, for pulse 13, despite the positive after-effects in NPI, no significant effects were measured on GS. Instead, the largest positive after-effect in GS were measured for pulse conditions 4, 8, 14, 16. 4, 8, and 14 are conditions where HE was significantly increased during pulse application, while 16 is a condition where HE changed initially in a negative direction, but then exhibited large positive after-effects. Looking more closely at the dynamics of GS evolution over the course of an experiment (Fig. S1), GS appears to increase through out the progression of the walking conditions for many of the pulse conditions on the group level. While many of the changes are not statistically significant at the individual pulse level (4), and so potential "drift" effects are smaller than the ones induced by specific torque pulse condition, the main effect of time point on GS indicates the that P-L, AE-E, and AE-L are all greater than baseline. This effect may be due in part to the participants not having reached a steady state walking speed on the user-driven treadmill, within the 100-150 strides of baseline..

Overall, the stepwise regression models indicate that the effects in propulsion mechanics measured after torque pulse application are associated with changes measured during pulse application, and that the nature of such an association is primarily of retention of training effects. Such retention seems to be primarily limited to the specific component of propulsion mechanics, whereby changes in HE after training are most strongly predicted by changes in HE during training, and so for NPI, TLA, and GS.

Some of the measured effects are in alignment with those measured previously in an experiment conducted at fixed walking speed [15]. In our previous work, we measured increased HE during training in conjunction with early stance extension and with late stance flexion torques, while a reversal in these torque directions led to decreased HE. In the user-driven treadmill training presented here, early pulse application effects were relatively attenuated but late application effects and after-effects were larger in magnitude and only positive. As per NPI, it had increased during training for flexion torques applied at late stance, and increased after training in conjunction with flexion torque pulses applied at early stance. In the user-driven treadmill training, only early stance extension torques, particularly at the knee, and late stance hip extension and knee flexion torques, exhibited strong positive effects in NPI during early pulse application. In agreement with the previous experiment, early stance flexion torques (pulse 8), particularly that which included the knee, exhibited significant positive after-effects in NPI. In addition, the user-driven treadmill experiment indicated has significant positive after-effects in NPI for late stance extension torques.

This study did have some limitations, that should be considered for future research in this topic. First, all participants held to the left handrail during the experiment. While this was consistent across all participants and pulse conditions, this factor may have introduced biomechanical constraints and/or effects to propulsive forces that have not been captured in the presented analyses. Moreover, the accuracy of the user-driven treadmill controller in identifying the participant's desired speed has not been quantified prior to this experiment. Specifically, the effect of several factors, such as the personal preference in being at the front or back of the treadmill, subject preference for a more/less responsive controller, effect of delay with respect to the lunge measurement, on the resultant behavior of the user-driven treadmill controller are likely complex. For both reasons, the results of this study are meaningful in a relative sense (comparison between torque conditions and different phased of torque pulse application within a gait cycle), but likely not in an absolute sense (i.e., change in GS, HE, NPI) when comparing to other studies using different experimental setups.

REFERENCES

[1] A. Middleton, S. L. Fritz, and M. Lusardi, "Walking speed: The functional vital sign," *J Aging Phys Act.*, vol. 23, no. 2, pp. 314–322, 2015.

[2] A. Schmid and E. al., "Improvements in Speed-Based Gait Classifications Are Meaningful," *Stroke*, vol. 38, pp. 2096–2101, 2007.

[3] L. N. Awad, H. Hsiao, and S. A. Binder-Macleod, "Central Drive to the Paretic Ankle Plantarflexors Affects the Relationship between Propulsion and Walking Speed after Stroke," *Journal of Neurologic Physical Therapy*, vol. 44, no. 1, pp. 42–48, 2020.

[4] C. L. Peterson, A. L. Hall, S. A. Kautz, and R. R. Neptune, "Pre-swing deficits in forward propulsion , swing initiation and power generation by individual muscles during hemiparetic walking," *Journal of Biomechanics*, vol. 43, no. 12, pp. 2348–2355, 2010.

[5] A. L. Hall, C. L. Peterson, S. A. Kautz, and R. R. Neptune, "Relationships between muscle contributions to walking subtasks and functional walking status in persons with post-stroke hemiparesis," *Clinical Biomechanics*, vol. 26, no. 5, pp. 509–515, 2011.

[6] C. L. Peterson, S. A. Kautz, and R. R. Neptune, "Braking and Propulsive Impulses Increase with Speed during Accelerated and Decelerated Walking," *Gait Posture*, vol. 33, no. 4, pp. 562–567, 2011.

[7] H. Hsiao, B. A. Knarr, J. S. Higginson, and S. A. Binder-Macleod, "The Relative Contribution of Ankle Moment and Trailing Limb Angle to Propulsive Force during Gait," *Human Mov. Sci.*, pp. 212–221, 2015.

[8] R. R. Neptune, F. E. Zajac, and S. A. Kautz, "Muscle force redistributes segmental power for body progression during walking," *Gait and Posture*, vol. 19, no. 2, pp. 194–205, 2004.

[9] C. L. Peterson, J. Cheng, S. A. Kautz, and R. R. Neptune, "Leg extension is an important predictor of paretic leg propulsion in hemiparetic walking," *Gait & Posture*, vol. 32, no. 4, pp. 451–456, 2010.

[10] H. Hsiao, B. A. Knarr, J. S. Higginson, and S. A. Binder-Macleod, "Mechanisms to increase propulsive force for individuals poststroke.," *Journal of Neuroengineering and Rehabilitation*, vol. 12, no. 40, 2015.

[11] A. J. Farrens, M. Lilley, and F. Sergi, "Training Propulsion via Acceleration of the Trailing Limb," *IEEE Transactions on Neural Systems and Rehabilitation Engineering*, vol. 28, no. 12, pp. 2816–2825, 2020.

[12] L. N. Awad, D. S. Reisman, T. M. Kesar, and S. A. Binder-macleod, "Targeting Paretic Propulsion to Improve Poststroke Walking Function : A Preliminary Study," *Archives of Physical Medicine and Rehabilitation*, vol. 95, no. 5, pp. 840–848, 2014.

[13] L. N. Awad, S. A. Binder-Macleod, R. T. Pohlig, and D. S. Reisman, "Paretic propulsion and trailing limb angle are key determinants of long-distance walking function after stroke," *Neurorehabilitation and Neural Repair*, vol. 29, no. 6, pp. 499–508, 2015.

[14] M. D. Lewek and G. S. Sawicki, "Trailing limb angle is a surrogate for propulsive limb forces during walking post-stroke," *Clinical Biomechanics*, 2019.

[15] R. McGrath, B. Bodt, and F. Sergi, "Robot-Aided Training of Propulsion during Walking: Effects of Torque Pulses Applied to the Hip and Knee Joints during Stance," *IEEE Transactions on Neural Systems and Rehabilitation Engineering*, vol. 28, no. 12, pp. 2923–2932, 2020.

[16] F. Porciuncula, T. C. Baker, D. Arumukhom Revi, J. Bae, R. Sloutsky, T. D. Ellis, C. J. Walsh, and L. N. Awad, "Targeting Paretic Propulsion and Walking Speed With a Soft Robotic Exosuit: A Consideration-of-Concept Trial," *Frontiers in Neurorobotics*, vol. 15, no. July, pp. 1–13, 2021.

[17] M. D. Lewek, C. H. Braun, C. Wutzke, and C. Giuliani, "The role of movement errors in modifying spatiotemporal gait asymmetry post stroke: a randomized controlled trial," *Clinical Rehabilitation*, vol. 32, no. 2, pp. 161–172, 2018.

[18] J. R. Franz, M. Maletis, and R. Kram, "Real-time feedback enhances forward propulsion during walking in old adults," *Clinical Biomechanics*, vol. 29, no. 1, pp. 68–74, 2014.

[19] M. G. Browne and J. R. Franz, "More push from your push-off: Joint-level modifications to modulate propulsive forces in old age," *Plos One*, vol. 13, no. 8, p. e0201407, 2018.

[20] L. N. Awad, J. Bae, P. Kudzia, A. Long, K. Hendron, K. G. Holt, K. ODonnell, T. D. Ellis, and C. J. Walsh, "Reducing Circumduction and Hip Hiking During Hemiparetic Walking Through Targeted Assistance of the Paretic Limb Using a Soft Robotic Exosuit," *American Journal of Physical Medicine & Rehabilitation*, vol. 00, no. 00, p. 1, 2017.

[21] P. Malcolm, W. Derave, S. Galle, and D. D. Clercq, "A Simple Exoskeleton That Assists Plantarflexion Can Reduce the Metabolic Cost of Human Walking," *Plos One*, vol. 8, no. 2, pp. 1–7, 2013.

[22] B. T. Quinlivan, S. Lee, P. Malcolm, D. M. Rossi, M. Grimmer, C. Siviy, N. Karavas, D. Wagner, A. Asbeck, I. Galiana, and C. J. Walsh, "Assistance magnitude versus metabolic cost reductions for a tethered multiarticular soft exosuit," *Science Robotics*, vol. 2, no. eaah4416, 2017.

[23] J. Zhang and E. al., "Human-in-the-loop optimization of exoskeleton assistance walking," *Science*, vol. 356, no. June, pp. 1280–1284, 2017.

[24] K. Genthe, C. Schenck, S. Eicholtz, L. Zajac-Cox, S. Wolf, and T. M. Kesar, "Effects of real-time gait biofeedback on paretic propulsion and gait biomechanics in individuals post-stroke," *Topics in Stroke Rehabilitation*, vol. 25, no. 3, pp. 186–193, 2018.

[25] V. Santucci, Z. Alam, J. Liu, J. Spencer, A. Faust, A. Cobb, J. Konantz, S. Eicholtz, S. Wolf, and T. M. Kesar, "Immediate improvements in post-stroke gait biomechanics are induced with both real-time limb position and propulsive force biofeedback," *Journal of NeuroEngineering and Rehabilitation*, vol. 20, no. 1, p. 37, 2023.

[26] J. Spencer, S. L. Wolf, and T. M. Kesar, "Biofeedback for post-stroke gait retraining: A review of current evidence and future research directions in the context of emerging technologies," *Frontiers in Neurology*, vol. 12, 2021.

[27] N. T. Ray, B. A. Knarr, and J. S. Higginson, "Walking speed changes in response to novel user-driven treadmill control," *Journal of Biomechanics*, vol. 78, pp. 143–149, 2018.

[28] K. N. Winfree, P. Stegall, and S. K. Agrawal, "Design of a minimally constraining, passively supported gait training exoskeleton: ALEX II," *IEEE ICORR*, pp. 0–5, 2011.

[29] T. Bihl, *Biostatistics Using JMP ® : A Practical Guide*. 2017.

[30] M. D. Lewek and G. S. Sawicki, "Trailing limb angle is a surrogate for propulsive limb forces during walking post-stroke," *Clinical Biomechanics*, vol. 67, pp. 115–118, 2019.